Mineral formation during bacterial sulfate reduction in the presence of different electron donors and carbon sources

Authors: Xiqiu Han, Logan Schultz, Weiyan Zhang, Jiahao Zhu, Fanxu Meng, & Gill G. Geesey

Han, Xiqiu, Logan Schultz, Weiyan Zhang, Jihao Zhu, Fanxu Meng, and Gill G. Geesey. "Mineral formation during bacterial sulfate reduction in the presence of different electron donors and carbon sources." Chemical Geology 435 (April 2016): 49-59. DOI: 10.1016/j.chemgeo.2016.04.022.

Mineral formation during bacterial sulfate reduction in the presence of different electron donors and carbon sources

Xiqiu Han[a], Logan Schultz[b], Weiyan Zhang[a], Jiahao Zhu[a], Fanxu Meng[c], & Gill G. Geesey[d]

[a] *Key Laboratory of Submarine Geosciences & The Second Institute of Oceanography, State Oceanic Administration, Hangzhou 310012, China*
[b] *Department of Chemical and Biological Engineering, Center for Biofilm Engineering, Montana State University, Bozeman, MT 59717-3980, United States*
[c] *Key Laboratory of Marine Ecosystem and Biogeochemistry & The Second Institute of Oceanography, State Oceanic Administration, Hangzhou 310012, China*
[d] *Thermal Biology Institute and Department of Microbiology, Montana State University, Bozeman, MT 59717-3520, United States*

Abstract

Sulfate-reducing bacteria have long been known to promote mineral precipitation. However, the influence of electron donors (energy sources) and carbon sources on the minerals formed during sulfate reduction is less well understood. An investigation was therefore undertaken to determine how these nutrients affect sulfate reduction by the bacterium *Desulfovibrio alaskensis* G20 in a marine sediment pore water medium. Monohydrocalcite and a small amount of calcite formed during sulfate reduction with formate as the electron donor; Mg-phosphates and calcite precipitated when hydrogen served as the electron donor and when acetate and dissolved inorganic carbon served as carbon sources; and greigite and elemental sulfur were deposited when lactate was used as the electron donor and carbon source. The experimental results were generally consistent with geochemical modeling, suggesting that it may be possible to predict the processes and conditions during formation of these minerals in natural environments.

Keywords: Carbonate; Monohydrocalcite; Marine cold seeps; Bacterial sulfate reduction; Electron donor

1. Introduction

Microorganisms are known to promote the precipitation of minerals (Bavendamm, 1932; Greenfield, 1963; Nadson, 1928). Sulfate-reducing bacteria (SRB) often contribute to the formation of carbonate minerals in marine and other sulfate containing saline environments (Breibart et al., 2009; Gunatilaka et al., 1984; Krause et al., 2012; Vasconcelos and McKenzie, 1997; Wright, 1997; Wright, 1999). For example, dolo-mite and Mg-calcite precipitate under hypersaline and moderately sa-line/brackish conditions, respectively, in the presence of SRB in highly reducing, organic C-rich coastal lagoons (Vasconcelos and McKenzie, 1997; Vasconcelos et al., 1995). Correspondingly, aragonite and Mg-calcite are common in marine cold seeps where the coupling of anaero-bic oxidation of methane and sulfate reduction favors their formation (Suess, 2014). Other carbonate phases such as (proto)-dolomite, sider-ite and ikaite (calcium carbonate hexahydrate) also occur under specific conditions at cold seep sites (Greinert and Derkachev, 2004; Han et al., 2004; Wang et al., 2014). Sulfate-reducing bacteria also promote precip-itation of phosphate-containing minerals (e.g. hydroxyapatite) under suboxic to anoxic conditions in ancient and modern upwelling systems (Alsenz et al., 2015; Arning et al., 2009; Schulz and Schulz, 2005).

Redox reactions associated with respiration and growth of SRB can lead to mineral formation (Birnbaum and Wireman, 1984; Da Silva et al., 2000; Douglas, 2005; Ferrer et al., 1988; Rivadeneyra et al., 2006; Sanchez-Roman et al., 2007; Vasconcelos and McKenzie, 1997; Wright, 1999). While it is well established that SRB-mediated changes in aqueous phase chemistry promote mineral formation, less is known about how electron donors and carbon sources for bacterial respiration and growth influence the process. Nevertheless, these metabolites play an important role in mineral precipitation (Dupraz and Visscher, 2005; Visscher et al., 1998; Warthmann et al., 2000).

Bacterial culture experiments, theoretical calculations and geochem-ical modeling have shown that pH, alkalinity and carbonate mineral sat-uration vary depending on the type of electron donor used for sulfate reduction but have not related results to the formation of specific m i n - erals (Gallagher et al., 2012). Other studies have shown that the con-sumption of a mixture of organic compounds and production of extracellular and cell wall material during sulfate reduction by Desulfovibrio alaskensis G20 (formerly D. desulfuricans G20, hereafter re-ferred to as G20) promoted the formation of calcite that differed in mor-phology from that formed abiotically, but did not determine how utilization of different carbon and energy sources influenced mineral-ogy and morphology (Bosak and Newman, 2005). The minerals formed during bacterial sulfate reduction may, however, offer insight to the electron donors used for the reaction in environments such as marine cold seeps where their identity remains elusive (McGlynn et al., 2015; Wegener et al., 2015).

Here we investigate the minerals formed when formate, hydrogen, or lactate serve as the electron donor for sulfate reduction by G20 in a medium chemically similar to marine sediment pore water from the sulfate–methane transition zone (SMTZ) of a marine cold seep system in the South China Sea where there is evidence of bacterial sulfate reduction and carbonate mineral formation (Suess, 2005). Since formate, hydrogen and lactate are found in cold seep sediments (Heuer et al., 2009; Kendall et al., 2007; Larowe et al., 2008), they may serve as electron donors for SRB in these systems.

G20 is a mutant strain of *D. desulfuricans* G100A that was isolated from an oil well (Wall et al., 1993; Weimer et al., 1988). This SRB was selected for the study because it has previously served as a model organism to study sulfate reduction and carbonate mineral precipitation in seawater (Bosak and Newman, 2003; Bosak and Newman, 2005). The metabolism of electron donors and carbon sources during sulfate reduction is also better understood in G20 than in other SRB known to be involved in the formation of natural mineral deposits (Hauser et al., 2011; Labrenz et al., 2000; Li et al., 2009; Li et al., 2011; Postgate, 1984; Price et al., 2014; van Lith et al., 2003; Weimer et al., 1988).

Lactate serves both as an electron donor for sulfate reduction and as a sole carbon source for growth of G20 (Li et al., 2009; Li et al., 2011; Postgate, 1984; Weimer et al., 1988). When formate serves as electron donor, both acetate and dissolved inorganic carbon (DIC) are required as carbon sources for cell growth since formate carbon is not assimilated by G20 (Li et al., 2009; Voordouw, 1995). Both acetate and dissolved inorganic carbon (DIC) are also required as carbon sources for growth of G20 when hydrogen serves as electron donor for sulfate reduction (Li et al., 2009; Voordouw, 1995). However, G20 does not use acetate as an electron donor for sulfate reduction (Weimer et al., 1988). Hydrogen also serves as a supplementary electron donor for G20 in formate and lactate medium, but only after the organic electron donor becomes limiting (Khosrovi et al., 1971). The results reported here suggest that the types of minerals formed in a marine sediment pore water medium offer insights into the reactions and conditions at the time of their formation.

2. Methods

2.1. Medium preparation, inoculation and incubation

The bacterial cultivation medium contained inorganic salts at concentrations found in sediment pore water at the SMTZ of a marine cold seep system in the South China Sea (Table 1). The exceptions were salts of ammonium (as NH_4Cl) and phosphate (as Na_2HPO_4) which were elevated to provide a sufficient amount of nitrogen and phosphorus for microbial growth. The medium also contained lactate, formate or acetate at a concentration higher than that reported in SMTZ pore water (Kendall et al., 2007) to allow sufficient sulfate reduction and cell growth for detectable mineral formation. The initial concentration of electron donor relative to electron acceptor (sulfate) favored electron acceptor (sulfate) limitation of sulfate reduction (i.e., exhaustion of electron acceptor before electron donor), while the initial concentration of the organic carbon source, nitrogen source and phosphorus source favored nitrogen-limited growth (i.e., exhaustion of NH_4Cl before Na_2HPO_4 and lactate or acetate), conditions known to exist in some carbonate mineral-forming environments (Joye et al., 2004). Wolf's vitamins were also added to the medium to support growth of G20 (Table 1).

All medium components except vitamins were prepared as a single solution. Hydrochloric acid was added to achieve a pH of 7.5 after autoclave sterilization. Wolf's vitamins were prepared as a concentrated solution as previously described (Atlas, 2004), filter-sterilized and aseptically added to the cooled sterile medium components.

The sterile acetate, formate or lactate medium (100 ml) was aseptically introduced to the autoclave-sterilized butyl rubber-stoppered serum bottles (120-ml vol), each containing an iron finishing nail (five bottles of each medium). The iron nail served as a substitute for the unknown form of naturally-occurring iron that reacts with soluble sulfide to form insoluble iron sulfides in cold seep sediments. The contents of the serum bottles were purged with a sterile stream of hydrogen for 1 h through the butyl rubber stopper to establish a reduction potential favoring sulfate reduction and to provide hydrogen as sole electron

Table 1
Chemical composition of pore water from sediment core S0177-GC 10 recovered from a depth of 5.1 m below the seafloor at a cold seep in the South China Sea and corresponding composition of the SRB cultivation medium.

Sediment pore water[a]		SRB cultivation medium				
Chemical species	Concentration	Chemical	Concentration		Chemical species	Concentration
	mmol/l		mg/l	mmol/l		mmol/l
I	0.024	I	3.05	0.024	I	0.024
NH_4	0.079	NH_4Cl	565.92	10.58	NH_4[b]	10.58
PO_4	0.014	Na_2HPO_4	126.34	0.89	PO_4[b]	0.89
Cl	555.8	NaCl	24,954.3	427.0	Cl	581.5
SO_4	22.3	Na_2SO_4	3160.2	22.3	SO_4	22.3
Br	0.86	KBr	102.6	0.86	Br	0.86
$Si(OH)_4$	0.43	Na_2SiO_3 $9H_20$	121.6	0.43	$Si(OH)_4$	0.43
B	0.44	$Na_2B_4O_7$	21.9	0.11	B	0.436
Mn	0.0011	$MnSO_4$ H_20	0.19	0.001	Mn	0.001
Ca	8.22	$CaCO_3$	6.2	0.062	Ca	8.22
Fe	0.00093	$FeCl_3$	0.15	0.0009	Fe	0.0009
Na	478	$NaHCO_3$	605	7.2	Na	575.7[c], 528.6[d]
Sr	0.085	$SrCl_2$ $6H_2O$	22.7	0.085	Sr	0.085
Ba	0.0004	$BaCO_3$	0.08	0.0004	Ba	0.0004
Li	0.023	Li_2CO_3	0.84	0.011	Li	0.023
K	10.7	KCl	733.5	9.8	K	10.7
Mg	50.7	$MgCl_2$ $6H_2O$	10,307.8	50.7	Mg	50.7
Alkalinity [mEq/l]	7.35	$CaCl_2$	905.6	8.16	Alkalinity	7.36[mEq/l]
H_2S mmol/l	345	Na-formate or	6405	94.2	CHO_2^-	94.2
		Na-acetate or	3854	47	$C_2H_3O_2^-$	47
		Na-lactate	5324	47	$C_3H_5O_3^-$	47
		Wolf's vitamin solution	1 ml/l			

[a] (Suess, 2005).
[b] The concentration has been adjusted to achieve a C:N:P ratio of 106:16:1.
[c] In formate containing medium, [Na] = 575.7 mM/l.
[d] In H_2 or lactate containing medium, [Na] = 528.6 mM/l.

donor for sulfate reduction in acetate medium. Like formate and lactate, the amount of hydrogen relative to sulfate in acetate medium favored depletion of electron acceptor before electron donor.

One bottle of each medium was used to assess the effects of medium preparation on pH and Ca and Mg concentration (t = 0). Two bottles of each medium were inoculated through the septum with two drops of a fresh culture of G20 using a hydrogen-purged syringe and needle and incubated at 25 °C for 10 months (t = 10 mo) to promote bacterial sulfate reduction. The two remaining bottles of each medium were incubated at the same temperature and period of time under sterile anaerobic conditions to serve as abiotic controls.

2.2. Analysis of aqueous phase

A 0.2-ml sample was collected from each bottle and centrifuged at 7300 × *g* for 10 min at 25 °C to pellet any suspended solids. A 0.1-ml subsample of the supernatant fraction was then diluted 1:100 with a solution consisting of 1% HNO_3 and 0.5% HCl using trace metal grade acids and the concentration of Ca and Mg measured by ICP-MS using an Agilent 7500c series instrument equipped with a Babington type nebulizer. A standard solution (Agilent, 5183-4688) containing a mixture of 25 elements was used in combination with internal standards (Li, Sc, Ge, Y, In, Bi) to calibrate the instrument to obtain the concentration of elements in the samples. The standard deviation among replicates of the standards was 4–8%. The pH and total alkalinity (TA) of the medium was measured using a Fisher Accument Model 825MP pH meter and a Mettler Toledo T50 alkalinity analyzer, respectively.

2.3. Analysis of solids

The medium in the bottles was filtered to collect solids which had formed during incubation. The solids retained on the filter were dried overnight at 30 °C in a nitrogen atmosphere and analyzed within a week of collection. The mineral phases were determined by X-ray diffraction (XRD) using a *Panalytical* X'Pert Pro MRD with Cu K-alpha radiation generated at 45 kV and 40 mA in 0.0167° per step in a 2θ angle interval between 5°and 70°. The Rietveld full-pattern fitting method was applied for quantitative mineralogical phase analysis.

The morphology and elemental composition of the solids were determined by scanning electron microscopy (SEM), energy-dispersive X-ray spectroscopic analysis (EDS) and electron microprobe analysis (EMPA). A subsample of the solid phase was transferred to a specimen holder, sputter-coated with platinum for 30 s at 20 mA using a JEOL JFC 1600 Auto Fine coater and examined using a Hitachi S-4800 scanning electron microscope with an Oxford X-MAX-20 energy-dispersive X-ray spectroscopic analysis system at an accelerating voltage of 15 kV. To assess the effect of coating, separate subsamples were deposited directly on silver foil and subjected to single particle elemental analysis without sputter-coating. Carbon sputter-coated samples were also analyzed using a JXA-8100 electron microprobe analyzer operated at an accelerating voltage of 15 kV, a beam current of 20 nA and a spot size less than 20 μm. The elemental composition of sample constituents obtained by EDS and EMPA was compared with that of known stoichiometric minerals available at http://webmineral.com to determine the possible mineral composition of the sample.

2.4. Chemical modeling

The program SpecE8 within the Geochemist's Workbench program version 10.0.4 (Rockware, Golden, Colorado, U.S.A.) employed the MINTEQ database (thermo_minteq.dat) to describe the SMTZ sediment pore water and the nutrient-enriched culture media, including the extent of complex formation involving the cations Ca^{2+} and Mg^{2+} and anions PO_4^{2-}, formate (CHO_2^-), acetate ($CH_3CO_2^-$) and lactate ($C_3H_5O_3^-$). Since the pH and organic acid concentrations were not measured in the SMTZ pore water of the South China Sea sediments, the program assumed a pH of 7.9 and that acetate, formate and lactate concentrations were the same as those measured in SMTZ pore water in cold seep sediments of Akan Bay, AK (Kendall et al., 2007).

The program React within the Geochemist's Workbench was used to simulate sulfate reduction and determine whether the observed mineral phases that formed during experiments are predicted on the basis of the measured changes in aqueous phase chemistry. The following reactions were used to describe sulfate reduction with each electron donor:

Hydrogen as electron donor in acetate medium (Meulepas et al., 2010):

$$4H_2 + SO_4^{2-} + H^+ \rightarrow HS\rightarrow + 4H_2O. \quad (1)$$

Formate as electron donor in formate medium (Meulepas et al., 2010):

$$4CHO_2^- + SO_4^{2-} + H_2O \rightarrow HS^- + 4HCO_3^- + OH^-. \quad (2)$$

Lactate as electron donor in lactate medium Oyekola et al., 2009:

$$2C_3H_5O_3^- + SO_4^{2-} \rightarrow 2C_2H_3O_2^- + HS^- + 2HCO_3^- + H^+. \quad (3)$$

The input values were based on the initial concentration of medium components provided in Table 1 after adjustments based on initial (t = 0) and final (t = 10 mo) measured elemental concentrations, pH and in some cases total alkalinity (SI Table 1). Although sulfate and sulfide concentrations were not measured in experiments, the model predicts changes in aqueous chemistry and mineral saturation for sulfate reduction from 0 to 100%. The model assumes a source of solid iron, which removes all soluble sulfide (as iron sulfide) during sulfate reduction (Bosak and Newman, 2003). Because minerals form during progressive sulfate reduction (and not only at the end), the model incorporates the precipitation of the primary minerals formed during sulfate reduction over a series of 10 steps: monohydrocalcite (MHC) in formate medium, hydroxyapatite in acetate medium, and greigite in lactate medium.

3. Results

3.1. Chemistry of aqueous solutions

Media inoculated with G20 experienced changes in aqueous phase chemistry that were different from those incubated under sterile anaerobic conditions. The pH increased from 7.5 to 8.3 in inoculated formate and acetate media, whereas it increased only slightly from 7.5 to 7.7 in uninoculated media (Table 2). The pH decreased from 7.5 to 6.9 in the inoculated lactate medium but increased from 7.5 to 8.0 when the medium was incubated under sterile conditions. The results demonstrate that the pH change is a function of the electron donor used for sulfate reduction, i.e. that lactate utilization decreases the pH, whereas formate and hydrogen utilization increases the pH.

Sulfate reduction with some electron donors also affected the precipitation of Ca and Mg through processes that could not be accounted for by abiotic reactions. In formate and acetate media, the Ca concentration decreased by 5.8 mM (67%) and 1.9 mM (22%), respectively, after 10 mo incubation, whereas no change in Ca concentration was observed in the lactate medium after incubation under sulfate-reducing conditions (Table 2, SI Fig. 1a). The Ca decrease in formate and acetate media could not be accounted for by abiotic reactions: Ca decreased by only 0.8 mM (9%) in the sterile formate medium and not at all in the sterile acetate medium after incubation for the same period of time (SI Fig. 1a). The Mg concentration decreased by 1.2 mM (2.3%) and 3.2 mM (5.9%) in the formate and acetate media, respectively, after 10 mo incubation under sulfate-reducing conditions (SI Fig. 1b). Since the Mg concentration did not decrease in the sterile formate medium, it is unlikely that abiotic reactions were responsible for the

Table 2
Chemical properties of media incubated under different conditions.

Condition	Medium	Rep_sample ID	pH	Ca (mM)[a]	Mg (mM)[a]	Total alkalinity (mmol/kg)	Contribution of specific mineral phases to total mineral content of solids (wt%)[b]	Contribution of amorphous phases to solids (wt%)	Weighted residual error of refinement (%)[c]	Expected residual error of refinement (%)[c]
Sterile, anaerobic, t = 0	Acetate	1_1	7.5	8.4	54.0	NA[d]	NA			
	Formate	1_2	7.5	8.5	53.5	NA	NA			
	Lactate	1_3	7.5	7.9	54.0	NA	NA			
Sterile, anaerobic, t = 10 mo	Acetate	1_105	7.7	8.1	49.9	NA	Calcite	89.4	2.75	4.32
		2_44	7.9	8.6	51.0	33.9	Calcite	89.4	3.25	2.8
	Formate[e]	1_47	7.7	7.7	53.5	13.4	Aragonite = 13.5, Mg-calcite ($Mg_{0.15}Ca_{0.85}CO_3$) = 29.8, quartz = 6.7	50.0	1.36	0.08
	Lactate	1_101	8.0	7.8	53.7	18.1	No mineral phase detected	100		
		2_50	8.0	7.7	50.8	NA	No mineral phase detected	100		
Sulfate reduction, t = 10 mo	Acetate	1_103	8.3	7.3	50.9	27.2	Baricite $(Mg,Fe)_3(PO_4)_2 \cdot 8H_2O$ = 30.6; Mg-phosphate hydrate $(Mg_3(PO_4)_2 \cdot 10H_2O$ = 48.7; calcite = 9.6, S_8 = 11.2	0	2.62	4.29
		2_35	8.3	5.8	50.2	NA	Baricite $(Mg,Fe)_3(PO_4)_2 \cdot 8H_2O$ = 27.8; Mg-phosphate hydrate $(Mg_3(PO_4)_2 \cdot 10H_2O$ = 56.2; calcite = 12.8, S_8 = 3.3	0	4.71	3.59
	Formate	1_38	8.3	2.7	50.6	NA	Monohydrocalcite = 98.4, calcite = 1.6	0	6.29	5.57
		2_104	8.4	2.8	52.3	43.4	Monohydrocalcite = 95.2, calcite = 4.8	0	6.72	5.74
	Lactate	1_41	6.9	7.9	52.8	18.0	Greigite (Fe_3S_4) = 76.0, S_8 = 24.0	97.0	5.09	4.1
		2_102	6.8	7.9	53.3	NA	Greigite (Fe_3S_4) = 52.8, S_8 = 47.2	96.9	1.74	9.16

[a] Concentration based on ICP-MS results.
[b] Identity based on XRD analysis.
[c] Residual error of refinement based on Rietveld full-pattern fitting method.
[d] NA; not analyzed.
[e] One of the replicate bottles containing the formate medium incubated under sterile conditions broke during shipment for analysis. Thus, data was generated from only one of the two replicates for this incubation condition.

decrease during sulfate reduction (SI Fig. 1b). By contrast, the decrease in Mg concentration in the sterile acetate medium (3.5 mM, 6.5%) was similar to that observed in the inoculated medium, suggesting that abiotic reactions may account for the decrease during sulfate reduction (SI Fig. 1b). As in the case of Ca, the Mg concentration in the lactate medium changed little during incubation under either biotic (0.9 mM, 1.7% decrease) or abiotic conditions (1.8 mM, 3.2% decrease) (SI Fig. 1b).

Sulfate reduction with some electron donors also affected alkalinity in ways that could not be accounted for by abiotic reactions. Following incubation, total alkalinity (TA) was higher in the inoculated than in the sterile formate medium (Table 2). By contrast, the TA was slightly lower after incubation of the inoculated than the sterile acetate medium (Table 2). These differences, albeit based on a single set of data, are consistent with results of other aqueous phase constituents which also varied depending on the electron donors used for sulfate reduction.

3.2. Solid characterization

All sterile media contained a trace of white solids prior to incubation under sterile anaerobic or sulfate-reducing conditions. A black precipitate appeared on the nail in all media inoculated with G20, indicating sulfide production and conversion to iron sulfide. Over the remaining 10-mo incubation period, the black precipitate accumulated throughout the inoculated lactate medium, but never extended beyond the nail in the inoculated formate and acetate media. No black precipitate appeared in media incubated for 10 mo under sterile conditions, indicating that sulfide production in the inoculated media was the result of biotic rather than abiotic reactions. During incubation, white solids continued to accumulate in the inoculated formate and acetate media but not in the inoculated lactate medium or any of the sterile media.

XRD results showed that the solids formed under the different conditions had different mineral compositions but replicates contained the same mineral phases (Table 3). Fig. 1 shows a typical XRD pattern from solids formed under each condition. The solids formed in the inoculated formate medium (1_38 and 2_104) consisted primarily of monohydrocalcite (MHC) and a small quantity of calcite (Fig. 1a, Table 2). The trace of white solids recovered from the formate medium incubated under sterile conditions (1_47) consisted of amorphous material, aragonite ($CaCO_3$), Mg-calcite ($Mg_{0.15}Ca_{0.85}CO_3$) and quartz (SiO_2) (Fig. 1b, Table 2). Thus, the minerals formed during bacterial sulfate reduction with formate differed from those that formed in the medium incubated under abiotic conditions.

The white solids that formed in the acetate medium after sulfate reduction with hydrogen (1_103 and 2_35) consisted of crystalline Mg-phosphate hydrate [$Mg_3(PO_4)_2 \cdot 10\ H_2O$], baricite [$(Mg, Fe^{2+})_3(PO_4)_2 \cdot 8\ H_2O$], calcite and S^o (Fig. 1c, Table 3). The trace of white solids recovered from the incubated sterile acetate medium (1_105 and 2_44) was comprised primarily of amorphous material with a small amount of calcite (Fig. 1d, Table 2). Thus, calcite was favored in the acetate medium in the presence and absence of sulfate reduction with hydrogen.

A small greigite (Fe_3S_4) and S^o were detected after sulfate reduction with lactate (1_41 and 2_102), whereas no mineral phase was detected in the sterile lactate medium (1_101 and 2_50) (Fig. 1e and f, Table 2). The solid phase formed under these conditions was dominated by amorphous material (Table 2).

SEM revealed that the solids from the inoculated formate medium were dominated by rhombohedral crystals in the size range of 2–7 μm (Fig. 2a). EDS analysis of samples containing only the crystals (1_38–7 & −8, 1_38–1-A & −8-A, 1_38–15-1 & −2, and 1_38_3–2) indicated that they consisted of C, O, Ca, with possibly traces of Mg in some instances (SI Table 2). The averaged Ca:C:O ratio of these samples was 0.7:1:3.2, typical of calcium carbonates. Small spheres of uniform size (~0.2 μm in diameter) were also observed in some samples (1_38–1-B, 1_38–3 through 1_38–6, 1_38–7-A through -D and 1_38–10 through

Table 3
EMPA-based chemical composition of minerals formed in formate medium under sulfate reducing condition.

Replicate_sample ID	CaO	SiO_2	Na_2O	MnO	SrO	MgO	FeO	SO_3	P_2O_5	Total	CO_2	H_2O	CO_2+H_2O[a]	Ca	Relative error	Mineral inferred
	wt%	wt%	wt%	wt%	wt%	wt%	wt%	wt%	wt%	wt%	wt%	wt%	wt%	at%	%[b]	
1_38–2	55.49	0.03	0.15	0.05	0.15	0.24	1.34	1.38	2.97	61.79	No data	No data	38.21	98.95	−1.05	Calcite
1_38–3	56.36	0.00	0.13		0.13	0.15	0.16	0.17	2.19	59.29	No data	No data	40.71	100.50	0.50	Calcite
1_38–4	55.21	–	0.01	0.02	0.07	0.09	0.12	0.27	2.59	58.38	No data	No data	41.62	98.45	−1.55	Calcite
1_38–1	43.51	0.10	0.09	0.10	0.14	0.43	1.21	0.42	3.37	49.35	No data	No data	50.65	77.59	−3.01	MHC
2_104–1	44.07	0.03	1.56		0.04	0.33	0.10	–	–	46.15	No data	No data	53.85	78.60	−1.76	MHC
2_104–2	45.58	0.05	0.62		0.07	0.06	0.01	–	–	46.41	No data	No data	53.59	81.27	1.59	MHC
2_104–3	45.96	0.03	0.56	0.03	0.05	0.05	0.18	0.36	1.49	48.71	No data	No data	51.29	81.96	2.45	MHC
2_104–4	46.00	0.03	0.16	0.07	0.06	0.08	–	0.25	1.57	48.23	No data	No data	51.77	82.03	2.54	MHC
2_104–5	46.48	–	0.34	0.08	0.15	0.21	0.03	0.06	1.23	48.59	No data	No data	51.42	82.89	3.61	MHC
Stoichiometric MHC	47.47										37.26	15.25	52.51	80		
Stoichiometric calcite	56.03										43.97		43.97	100		

Precision was better than 3% for major elements and 5–10% for minor elements based on repeated analysis of standards.

[a] Because C and O were not determined by EMPA, it was assumed that CO_2 and $CO_2 + H_2O$ made up the difference between 100% and the total contents of oxides for calcite and monohydrocalcite, respectively.

[b] Relative error as %, which was calculated from the atomic percentage of Ca in the samples relative to Ca in corresponding stoichiometric mineral according to the equation $[Ca_{measured} - Ca_{stoichiometric}] / Ca_{stoichiometric}] \times 100$. Elemental composition of stoichiometric minerals was obtained at http://webmineral.com.

12) as aggregations or chains adjacent to the rhombohedral crystals (Fig. 2b). The spheres have a rough surface texture and appear to be hollow based on the voids observed within a few of the spheres that were broken or had holes in their surface (Fig. 2c & d). Since the spheres were smaller than the smallest interaction volume (~ 6–9 μm^3) sampled by EDS (Kanaya and Okayama, 1972), their elemental composition was assessed by focusing the electron beam on aggregations of spheres, which together with the crystals made up the total sample volume. All sampled volumes with both spheres and crystals contained mostly Ca, C and O, with Mg, often Fe, occasionally P and possibly a trace of Na, Si and Cl present (SI Table 2). However, the atomic percentages did not match any known stoichiometric minerals.

Extensive SEM of solids recovered from the formate medium incubated under sterile conditions revealed no morphologies characteristic of the aragonite or Mg-calcite detected by XRD. Presumably, these minerals were obscured by the large amount of amorphous material present (Table 2). However, many of the samples contained hollow spheres with a smooth surface and a wider range of sizes (0.4–2.5 μm dia.) than the spheres observed in the inoculated medium (Fig. 3a and b). EDS indicated that all sampled volumes with spheres contained mostly C and O, lesser amounts of Mg, Ca, Fe, P and possibly a trace of Na and Si (SI Table 2). The atomic percentages did not match any known stoichiometric minerals, presumably due to interference from amorphous material present in the samples.

The amorphous material which dominated the solids in the incubated sterile acetate medium and the inoculated lactate medium also obscured the calcite, greigite and sulfur detect in the respective media by XRD. SEM examination of solids from inoculated acetate medium revealed crystals with morphologies corresponding to the phosphate minerals detected by XRD (data not shown), but were not further characterized.

Since MHC and calcite do not typically coexist under conditions in which microorganism are present (Davies et al., 1977; Fischbeck and Müller, 1971), the solids from the inoculated formate medium were examined further by EMPA to learn more about the composition of these polymorphs. The CaO content varied from 43.5 to 46.0 wt% in some samples (1_38–1 and 2_104–1 to −5) and from 55.2 to 56.4 wt% in other samples (1_ 38–2 to −5) (Table 3). MgO, FeO, Na_2O, P_2O_5, SrO and SO_3 were present in minor or trace amounts. The total amount of oxides range from 46.2 to 61.8 wt%. It was assumed that CO_2 and CO_2 plus H_2O accounted for the balance of C and O for calcite and MHC, respectively, since C and O were not determined by EMPA. The calculated atomic percentages of Ca and CO_2 and Ca and ($CO_2 + H_2O$) correspond to that of stoichiometric calcite and MHC, respectively (Table 3). The slightly positive and negative percent relative error for the atomic percentage of Ca indicates that the minerals may contain trace of Mg (<0.01 mol%) and some other elements but still possess close to the ideal Ca stoichiometry for MHC and calcite, respectively, thus supporting the XRD results that both of these calcium carbonate polymorphs formed during sulfate reduction with formate.

In summary, bacterial sulfate reduction promoted precipitation of minerals different from those which formed in sterile medium. The use of different electron donors for sulfate reduction favored the precipitation of different minerals: carbonates when formate served as electron donor, predominantly phosphates and a small amount of carbonate when hydrogen served as electron donor and sulfur-containing minerals when lactate served as electron acceptor.

3.3. Modeling of experiments

The predictions of the geochemical model generally agreed with experimental data, assuming the sulfate-reducing reactions presented in (Eqs. (1)–(3)). The trace amount of white precipitates in all media prior to incubation is consistent with the modeled prediction of slight supersaturation with respect to calcium phosphate [$Ca_3(PO_4)_2$], hydroxyapatite [Ca (PO4) (OH)], dolomite [$CaMg(CO_3)_2$], and calcite ($CaCO_3$) based on the concentrations of media components (SI Fig. 2). The predicted pH increase from 7.5 to 8.7 and from 7.5 to 8.4 upon reduction of all the sulfate to sulfide in the formate and acetate media, respectively, was similar to the increase measured in the experiments (SI Fig. 3). Correspondingly, the pH decrease predicted by the model upon reduction of sulfate in the lactate medium reflected the measured decrease after incubation of the inoculated medium (SI Fig. 3). Thus, the changes in pH observed after incubation of all inoculated media are consistent with those attributable to sulfate reduction according to Eqs. (1–3).

Model predictions of changes in the SI of various mineral phases during sulfate reduction with different electron donors were generally consistent with the behavior of Ca and Mg in the experiment. When the model reacted the 5.8 mM of Ca lost from solution during the 10-mo incubation with a stoichiometric amount of carbonate under sulfate-reducing conditions using formate as electron donor, calcite and MHC were supersaturated after 10% of the sulfate in the medium had been reduced (SI Fig. 2). When the model reacted the experimental Ca decrease of 1.9 mM with stoichiometric amounts of phosphate and hydroxide to form hydroxyapatite under sulfate-reducing conditions with hydrogen as electron donor, the SI of hydroxyapatite was predicted to be lower after all the sulfate was consumed than before sulfate reduction (SI Fig. 2). The predicted decrease in the SI of hydroxyapatite during later stages of sulfate reduction agrees with the experimental result: its absence from the medium after incubation. The experimental detection

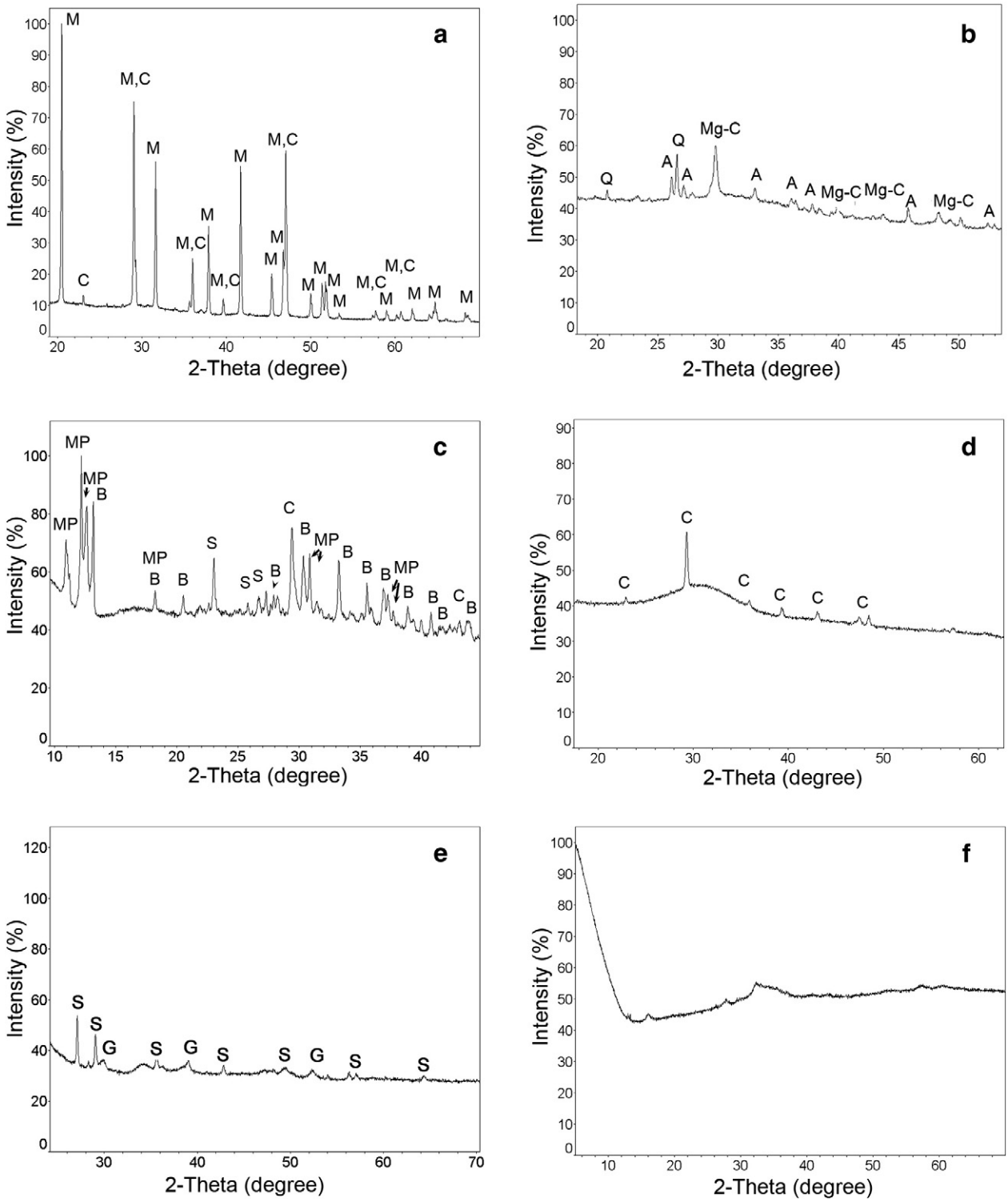

Fig. 1. XRD spectrum of solids formed in one of the incubated replicates of formate medium under a) sulfate-reducing and b) sterile anaerobic conditions; acetate medium under c) sulfate-reducing and d) sterile anaerobic conditions; lactate medium under e) sulfate-reducing and f) sterile anaerobic conditions. Note, M = monohydrocalcite, Q = quartz, A = aragonite, Mg-C = Mg-calcite, C = calcite, MP = $Mg_2(PO_4)_3 \cdot 10H_2O$, B = Baricite [$(Mg, Fe^{2+})_3 (PO_4)_2 \cdot 8H_2O$], S = elemental sulfur, G = greigite.

of $Mg_3(PO_4)_2$ also agrees with the model prediction of supersaturation under these conditions (SI Fig. 2).

A smaller increase in the SI of carbonates was predicted during sulfate reduction with hydrogen compared to formate (SI Fig. 2), agreeing with XRD results that carbonate minerals contributed a smaller fraction of the solids formed with hydrogen than formate as electron donor (Table 2). The extent to which various minerals precipitated during sulfate reduction with the different electron donors generally followed model predictions. The smaller increase in SI predicted for carbonates during sulfate reduction with hydrogen than with formate (SI Fig. 2) is accordant with XRD results indicating that carbonate minerals contributed a smaller fraction of the solids formed under the former than under the latter conditions (Table 2). Similarly, the model predicted a decrease in the SI of $Ca_3(PO_4)_2$ and only small changes in the SI of other phosphate and

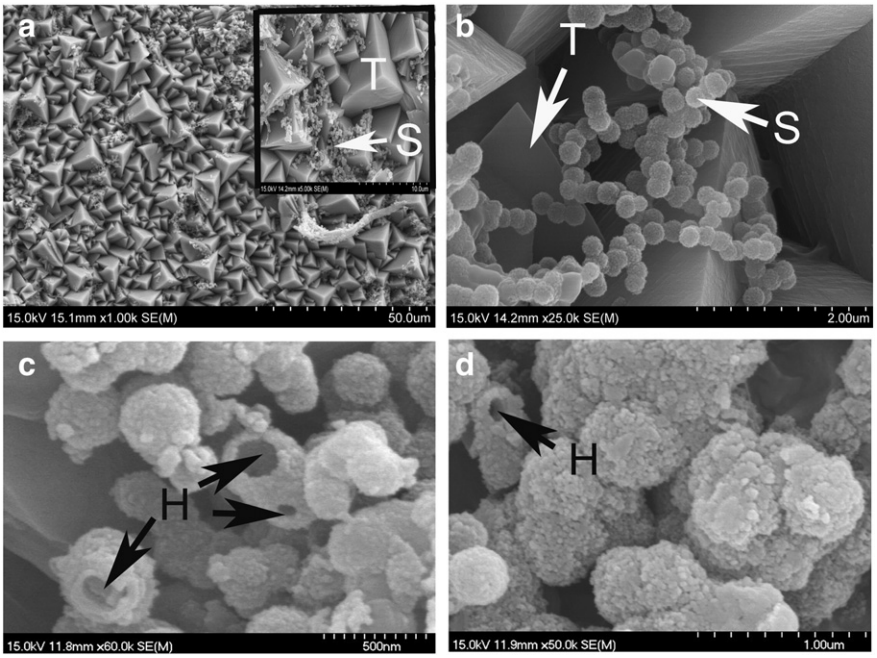

Fig. 2. Morphology and structure of solids that precipitated in formate medium incubated under sulfate-reducing conditions (Rep 1_Sample 38); a) low magnification SEM image of solids with inset showing enlargement of rhombohedral crystals (T) and associated spheres (S); b) higher magnification image of solids showing morphology and arrangement of spheres (S); c) high magnification view showing holes (H) in some spheres; d) higher magnification view showing surface texture of spheres.

carbonate minerals after sulfate reduction with lactate (SI Fig. 2); consistent with the absence of phosphate and carbonate minerals in the experiment.

The model also predicted that among the three electron donors used in this study, sulfate reduction with formate produced the largest increase in carbonate alkalinity (CA) after all sulfates were reduced. The experimental TA results supported this prediction. The model predicted a small increase in CA after reduction of all sulfates when hydrogen served as electron donor; however, the TA decreased slightly under these experimental conditions. Nevertheless, the model generally supported the experimental data indicating that mineral precipitation is influenced by the electron donor, according to changes to fluid chemistry based on the reactions in Eqs. (1–3).

4. Discussion

4.1. Abiotic reactions among medium components

All but one of the media used in the study supported mineral formation under sterile anaerobic conditions. The formation of aragonite and Mg-calcite but not calcite in the formate medium is consistent with other studies showing that high initial sulfate and phosphate concentrations, high Mg/Ca ratios and low calcite supersaturation favor the formation of other polymorphs of calcium carbonate over calcite (Berner, 1975; De Choudens-Sanchez and Gonzalez, 2009; Gallagher et al., 2013; Mucci and Morse, 1983; Rivadeneyra et al., 1985; Rodriguez-Blanco et al., 2014; Taylor, 1975; Tracy et al., 1998). The increase in the Mg/Ca ratio observed during incubation likely contributed to calcite inhibition. Aragonite and Mg-calcites are common carbonate minerals at marine cold seeps (Greinert and Derkachev, 2004; Han et al., 2008; Han et al., 2004). Thus, in spite of the unnaturally high concentrations of ammonia, phosphate and formate in the medium, the incubation conditions were sufficiently similar to those in marine cold seep sediments to favor precipitation of the same dominant mineral phases. While the formation of these minerals at marine cold seeps has been attributed to the anaerobic oxidation of methane by microorganisms (Boetius et al., 2000; Greinert and Derkachev, 2004; Han et al., 2008; Han et al., 2004; Paull et al., 1992; Suess et al., 1999), the results here suggest that they can also form abiotically in nutrient-enriched pore water medium containing formate.

The formation of calcite when acetate replaced formate in the medium suggests that the initial high sulfate and phosphate concentrations, high Mg/Ca ratio and low calcite supersaturation were not sufficient to inhibit its formation under these conditions. Since Mg is

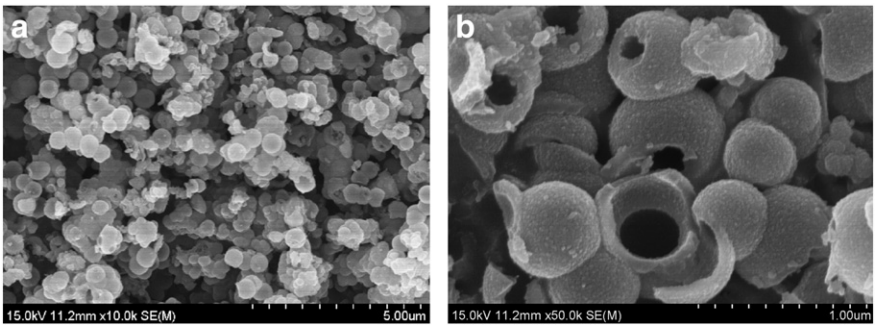

Fig. 3. Morphology and structure of solids that precipitated in formate medium incubated under sterile anaerobic conditions (Rep 1_Sample 47); a) low magnification SEM image of hollow spheres; b) high magnification SEM image showing surface texture of hollow spheres.

known to inhibit calcite formation (Bischoff and Fyfe, 1968; Cölfen, 2003; De Choudens-Sanchez and Gonzalez, 2009; Morse et al., 2007), the precipitation of Mg and accompanying decrease in the Mg/Ca ratio during incubation of the acetate medium likely allowed calcite to form under these conditions. By contrast, the inhibition of Ca and Mg precipitation by lactate likely prevented mineral formation under sterile conditions when it replaced formate or acetate in the medium.

The difference in removal of Ca and Mg from sterile anaerobic formate, acetate and lactate media may reflect variations in the extent to which Ca and Mg interact with these organic compounds, since the composition of the media differed only with respect to these components. The formation of soluble complexes changes the solution activity of Mg and Ca and thus the SI of minerals containing these cations (Fein, 1991). According to the geochemical model, formate complexed more Ca and Mg than did lactate and acetate, indicating that higher concentrations and saturation values are predicted for Ca and Mg minerals in the acetate and lactate media than in the formate medium (SI Table 2). Thus, more Ca and Mg should have precipitated in the lactate and acetate media than in the formate medium, contrary to what was observed experimentally. The model also indicated that formate complexed more Ca than Mg, favoring precipitation of Mg over Ca (SI Table 2), again contradicting the experimental results. The model further indicated that acetate complexed more Mg than Ca (SI Table 2), which should have favored an increase in the Mg/Ca ratio and inhibition of calcite, in contrast to what was observed in the experiment. Thus, the predicted complexation of Ca and Mg by acetate cannot account for alleviation of calcite inhibition in acetate medium. Instead, the results suggest that processes other than the complexation reactions considered here controlled the abiotic precipitation of Ca and Mg in formate, acetate and lactate media. Nevertheless, the results are consistent with those of other studies indicating that the type of carbonate mineral formed in various media depends on the organic constituents present in solution (Berner, 1975; Kitano and Hood, 1965; Mann et al., 1990; Meldrum and Hyde, 2001; Suess, 1970; Zullig and Morse, 1988).

4.2. Changes in medium composition during bacterial sulfate reduction

The observed increase in medium pH during sulfate reduction with formate and hydrogen results from the consumption of protons during the oxidation of these electron donors, the removal of sulfate from solution and the removal of hydrogen sulfide by the iron in the medium (Ben-Yaakov, 1973; Castanier et al., 1999; Hockin and Gadd, 2007; Stoessell, 1992; Thauer et al., 2009; Wright, 1999). The decrease in medium pH when lactate serves as electron donor has been attributed to the formation of acetic acid and the production and accumulation of protons in the medium after sulfate become limiting (Birnbaum and Wireman, 1984; Pankhania et al., 1988; Plugge et al., 2011). In the present study, the pH of the medium decreased even though protons produced by the reactions above were consumed through oxidation of the nail to Fe(II) during the formation of iron sulfide (Castanier et al., 1999; Enning and Garrelfs, 2014).

The increase in TA during sulfate reduction with formate was consistent with model predictions of an increase in CA and with the results of others (Gallagher et al., 2012). Alkalinity increases when DIC is produced from the oxidation of organic electron donors and when sulfate is removed during sulfate reduction (Abd-le-Malek and Rizk, 1963; Larowe et al., 2008; Meister, 2013). According to Eq. (1), DIC is produced during formate oxidation. The slight decrease in TA with hydrogen as electron donor in acetate medium likely reflects consumption of more alkalinity from growth-related removal of DIC from solution (supplied in the form of carbonate medium components) than that generated by sulfate removal. The discrepancy between the slight decrease in TA of the medium observed under these conditions and the slight increase in CA predicted by the model likely results from the model not accounting for cell growth-related DIC consumption as neither growth nor DIC concentration were measured in the study.

The changes in calcite SI ($SI_{calcite}$) during sulfate reduction with formate, hydrogen or lactate that were predicted by the model followed the trends observed in other modeling studies (Gallagher et al., 2012). The higher $SI_{calcite}$ predicted during sulfate reduction with formate than with hydrogen likely reflected the difference in TA since pH changes were similar under both conditions. The decrease in $SI_{calcite}$ predicted at the onset of sulfate reduction with lactate is thought to result from acid production, while the return to near initial values later in the incubation has been attributed to bicarbonate production (Gallagher et al., 2012).

4.3. Mineral precipitation during sulfate reduction

Although the model indicated that dolomite, $Ca_3(PO_4)_2$, $Ca_4(PO_4)_3 \cdot 3H_2O$, $Mg_3(PO_4)_2$, MHC and calcite were all supersaturated during sulfate reduction in formate medium, MHC and a small amount of calcite were the only mineral phases detected under these conditions. MHC typically precipitates as a secondary mineral in the presence of microorganisms (Davies et al., 1977; Rivadeneyra et al., 1998; Rivadeneyra et al., 1993; Rivadeneyra et al., 2004). Small quantities of MHC have been reported to precipitate with nonstoichiometric dolomite during sulfate reduction with formate in a medium simulating conditions of a hypersaline lagoon (Warthmann et al., 2000). However, this is the first time the precipitation of MHC was favored over other $CaCO_3$ polymorphs under sulfate-reducing conditions.

While MHC and calcite have similar structures, both belonging to the rhombohedral subclass (trigonal) of the hexagonal system (Dahl and Buchardt, 2006; Roberts et al., 1990), the large rhombohedral crystals seen by SEM dominating the solid phase in the inoculated formate medium are likely MHC because it contributed the bulk (96%) of the crystalline material in the sample. The low Mg content of the large MHC crystals observed here suggests that they were at an advanced stage of development since Mg is released during the maturation process (Rodriguez-Blanco et al., 2014). While the transformation of metastable MHC to calcite has been described under abiotic conditions (Liu et al., 2013), investigation of this process under bacterial sulfate-reducing conditions here was beyond the scope of the present study.

MHC typically precipitates with other carbonates such as Mg-calcite, aragonite, Ca-rich dolomite, hydromagnesite and nesquehonite under conditions of calcite inhibition (Broughton, 1972; Fischbeck and Müller, 1971; Nishiyama et al., 2013; Rodriguez-Blanco et al., 2014; Taylor, 1975; Warthmann et al., 2000). The increase in TA and pH during sulfate reduction with formate, conditions which are known to favor carbonate precipitation (Braissant et al., 2003; Davies et al., 1977; Ganendra et al., 2014; Hammes and Verstraete, 2002; Meister, 2013; Taylor, 1975; Warthmann et al., 2000), likely favored MHC formation in the medium. The importance of the TA increase to MHC formation was evident since the mineral did not form during sulfate reduction with hydrogen in acetate medium which produced in a similar increase in pH without an accompanying increase in TA.

The high TA achieved during sulfate reduction in the formate medium may also have inhibited phosphate precipitation as shown in previous studies (Ferguson et al., 1973). Thus, products of electron donor oxidation formed during bacterial sulfate reduction control the precipitation of phosphate as well as carbonate minerals through their influence on alkalinity. The inhibition of phosphate precipitation by high TA, the inhibition of calcite and aragonite by phosphate and organic compounds (Dahl and Buchardt, 2006), and the enhancement of phosphate inhibition of calcite and aragonite by sulfate removal (Burton, 1993) all likely favored MHC formation during sulfate reduction with formate. The unnaturally high phosphate concentration used to promote SRB growth in the present study may therefore have favored MHC formation over aragonite and Mg-calcite, the polymorphs which typically dominate carbonate deposits at marine cold seeps.

Although MHC has not been found at marine cold seeps, it is a common mineral (up to 55%) in debris fragments from submarine ikaite

($CaCO_3$. $6H_2O$) tufa columns in the marine Ikka fjord in southwestern Greenland (Dahl and Buchardt, 2006). In this environment MHC is thought to be a transitional diagenetic phase in the recrystallization of ikaite to calcite, similar to glendonite, an ikaite pseudomorph found at marine cold seeps (Greinert and Derkachev, 2004). The conditions which favored MHC formation in the fjord system (high phosphate, alkalinity and Mg/Ca ratio and low sulfate in a confined pore water system) are similar to those which favored its formation in the present study. Thus, bacterial sulfate reduction with formate has the potential to establish conditions favoring MHC formation in marine systems where ikaite, high phosphate concentrations and high Mg/Ca ratios exist.

The precipitation of phosphate minerals during microbial sulfate reduction has been attributed to the high concentration of phosphate in the cultivation medium to promote growth of SRB (Gallagher et al., 2013). Although the high phosphate concentration likely favored the precipitation of phosphate minerals during sulfate reduction in the acetate medium, other factors also contributed to their precipitation under these conditions since no phosphate minerals precipitated during sulfate reduction in the formate or lactate media, which contained the same initial phosphate concentrations. The slight decrease in TA and presumed consumption of DIC as a carbon source for growth of G20, which did not occur during sulfate reduction in formate and lactate media, also favored phosphate mineral formation in the acetate medium. Indeed, preliminary experiments indicated that the white solids, including phosphate minerals, did not accumulate during sulfate reduction with hydrogen unless acetate was present in the medium to support cell growth.

Although not measured, the phosphate concentration would have decreased during sulfate reduction in the acetate medium as a result of phosphate mineral formation. Since calcite growth is affected by phosphate concentration (Burton, 1993; Burton and Walter, 1990; Reddy, 1977), precipitation of phosphate may have alleviated calcite inhibition even though the accompanying increase in the Mg/Ca ratio from 6.6 to 8.1 favored inhibition. The results are consistent with those of previous studies indicating that multiple factors often contribute to calcite precipitation (De Choudens-Sanchez and Gonzalez, 2009; Fernandez-Diaz et al., 1996; Given and Wilkinson, 1985).

Greigite and sulfur were the only minerals that precipitated during sulfate reduction with lactate as electron donor. These phases likely occurred instead of carbonate minerals because of the reduction in pH (Abbona et al., 1982; Birnbaum and Wireman, 1984; Stoessell, 1992). While the SI of greigite was not modeled here, the pH change predicted by the model mimicked the pH change that occurred in the lactate medium. The formation of iron sulfides at low pH during sulfate reduction with lactate and at high pH during sulfate reduction with formate and hydrogen agrees with other studies (Donald and Southam, 1999). Greigite and elemental sulfur are among the sulfur minerals found at marine cold seeps within or near the SMTZ where their formation is thought to result from the activities of SRB (Lin et al., 2015; Wrede et al., 2013).

4.4. Conclusions

The findings reported here show that bacterial sulfate reduction with different electron donors results in the formation of different minerals in response to chemical changes in the medium associated with the consumption and production of reactants and products of the redox reactions. MHC and calcite formed during the oxidation of formate, Mg-phosphates, baricite, calcite and elemental sulfur formed during the oxidation of hydrogen and greigite and elemental sulfur formed during the oxidation of lactate. The results support a growing body of evidence that the types of minerals formed in the presence of microorganisms are influenced by the metabolic pathway used for energy production and growth (Visscher and Stolz, 2005). Thus, the MHC observed in a coastal fjord system may have formed through sulfate reduction with formate since some of the conditions in that environment resemble those generated by this process in the present study. The inability to promote formation of the common carbonate minerals found at marine cold seeps in the studies reported here may have been due to the high phosphate concentration used in the experiments and the current uncertainty of the electron donor used by SRB inhabiting the SMTZ.

Supplementary data to this article can be found online at http://dx.doi.org/10.1016/j.chemgeo.2016.04.022.

Acknowledgments

This study was funded by National Natural Science Foundation of China (No. 40976040), 973 Program (2009CB21950607), Zhejiang Provincial National Natural Science Foundation of China (No. R5110215), and the US Department of Energy (No. DE-FG02-13ER86571). Funding for the establishment and operation of the Environmental and Biofilm Mass Spectrometry Facility at Montana State University (MSU) was provided by the Defense University Research Instrumentation Program (DURIP, Contract Number W911NF0510255) and the MSU Thermal Biology Institute from the NASA Exobiology Program (Project NAG5-8807). We would like to thank Prof. Erwin Suess for his constructive discussions.

References

Abbona, F., Lundagger Madsen, H.E., Boistelle, R., 1982. Crystallization of two magnesium phosphates, struvite and newberyite: Effect of pH and concentration. J. Cryst. Growth 57 (1), 6–14.
Abd-le-Malek, Y., Rizk, S.G., 1963. Bacterial sulphate reduction and the development of alkalinity I. Experiments with synthetic media. J. Appl. Bacteriol. 26 (1), 7–13.
Alsenz, H., et al., 2015. Geochemical evidence for the link between sulfate reduction, sulfide oxidation and phosphate accumulation in a late cretaceous upwelling system. Geochem. Trans. 16, 1–13.
Arning, E.T., Birgel, D., Brunner, B., Peckmann, J., 2009. Bacterial formation of phosphatic laminites off Peru. Geobiology 7 (3), 295–307.
Atlas, R.M., 2004. Handbook of Microbiological Media. CRC Press, Boca Raton, FL.
Bavendamm, W., 1932. Die mikrobiologische Kalkfallung in der tropischen See. Arkiv. Mikrobiol. 3, 205–276.
Ben-Yaakov, S., 1973. pH buffering of pore water of recent anoxic marine sediments. Limnol. Oceanogr. 18 (1), 86–94.
Berner, R.A., 1975. The role of magnesium in the crystal growth of calcite and aragonite from sea water. Geochim. Cosmochim. Acta 39 (4), 489–504.
Birnbaum, S.J., Wireman, J.W., 1984. Bacterial sulfate reduction and pH: implications for early diagenesis. Chem. Geol. 43 (1–2), 143–149.
Bischoff, J.L., Fyfe, W.S., 1968. Catalysis, inhibition, and the calcite-aragonite problem. Am. J. Sci. 266 (2), 65–79.
Boetius, A., et al., 2000. A marine microbial consortium apparently mediating anaerobic oxidation of methane. Nature 407 (6804), 623–626.
Bosak, T., Newman, D.K., 2003. Microbial nucleation of carbonate on bacterial nanoglobules. Geology 31 (7), 577–580.
Bosak, T., Newman, D.K., 2005. Microbial kinetic controls on calcite morphology in supersaturated solutions. J. Sediment. Res. 75 (2), 190–199.
Braissant, O., Cailleau, G., Dupraz, C., Verrecchia, A.P., 2003. Bacterially induced mineralization of calcium carbonate in terrestrial environments: the role of exopolysaccharides and amino acids. J. Sediment. Res. 73, 485–490.
Breibart, M., et al., 2009. Metagenomic and stable isotope analysis of modern freshwater microbialites in Cuatro Cienegas Mexico. Environ. Microbiol. 11 (1), 16–34.
Broughton, P.L., 1972. Monohydrocalcite in speleothems: an alternative interpretation. Contrib. Mineral. Petrol. 36 (2), 171–174.
Burton, E.A., 1993. Controls on marine carbonate cement mineralogy: review and reassessment. Chem. Geol. 105 (1–3), 163–179.
Burton, E.A., Walter, L.M., 1990. The role of pH in phosphate inhibition of calcite and aragonite precipitation rates in seawater. Geochim. Cosmochim. Acta 54 (3), 797–808.
Castanier, S., Le Metayer-Levrel, G., Perthuisot, J.P., 1999. Ca-carbonates precipitation and limestone genesis-the microbiologists point of view. Sediment. Geol. 126 (1–4), 9–23.
Cölfen, H., 2003. Precipitation of carbonates: recent progress in controlled production of complex shapes. Curr. Opin. Colloid Interface Sci. 8 (1), 23–31.
Da Silva, S., Bernet, N., Delgenes, J.P., Moletta, R., 2000. Effect of culture conditions on the formation of struvite by *Myxococcus xanthus*. Chemosphere 40 (12), 1289–1296.
Dahl, K., Buchardt, B., 2006. Monohydrocalcite in the arctic ikka fjord, sw greenland: first reported marine occurrence. J. Sediment. Res. 76 (3), 460–471.
Davies, P.J., Bubela, B., Ferguson, J., 1977. Simulation of carbonate diagenetic processes: formation of dolomite, huntite and monohydrocalcite by the reactions between nesquehonite and brine. Chem. Geol. 19 (1–4), 187–214.
De Choudens-Sanchez, V., Gonzalez, L.A., 2009. Calcite and aragonite precipitation under controlled instantaneous supersaturation: elucidating the role of $CaCO_3$ saturation state and Mg/Ca ratio on calcium carbonate polymorphism. J. Sediment. Res. 79 (6), 363–376.

Donald, R., Southam, G., 1999. Low temperature anaerobic bacterial diagenesis of ferrous monosulfide to pyrite. Geochim. Cosmochim. Acta, 63 (13–14): 2019–2023.

Douglas, S., 2005. Mineralogical footprints of microbial life. Am. J. Sci. 305 (6–8), 503–525.

Dupraz, C., Visscher, P.T., 2005. Microbial lithification in marine stromatolites and hypersaline mats. Trends Microbiol. 13 (9), 429–438.

Enning, D., Garrelfs, J., 2014. Corrosion of iron by sulfate-reducing bacteria: new views of an old problem. Appl. Environ. Microbiol. 80 (4), 1226–1236.

Fein, J.B., 1991. Experimental study of aluminum-, calcium-, and magnesium-acetate complexing at 80 °C. Geochim. Cosmochim. Acta 55 (4), 955–964.

Ferguson, J.F., Jenkins, D., Eastman, J., 1973. Calcium phosphate precipitation at slightly alkaline pH values. J. Wat. Pollut. Contr. Fed. 45 (4), 620–631.

Fernandez-Diaz, L., Putnis, A., Prieto, M., Putnis, C.V., 1996. The role of magnesium in the crystallization of calcite and aragonite in a porous medium. J. Sediment. Res. 66 (3), 482–491.

Ferrer, M.R., et al., 1988. Calcium-carbonate formation by *Deleya halophila* - effect of salt concentration and incubation temperature. Geomicrobiol J. 6 (1), 49–57.

Fischbeck, R., Müller, G., 1971. Monohydrocalcite, hydromagnesite, nesquehonite, dolomite, aragonite, and calcite in speleothems of the Fränkische Schweiz, Western Germany. Contrib. Mineral. Petrol. 33 (2), 87–92.

Gallagher, K.L., Kading, T.J., Braissant, O., Dupraz, C., Visscher, P.T., 2012. Inside the alkalinity engine: the role of electron donors in the organomineralization potential of sulfate-reducing bacteria. Geobiology 10 (6), 518–530.

Gallagher, K.L., Braissant, O., Kading, T.J., Dupraz, C., Visscher, P.T., 2013. Phosphate-related artifacts in carbonate mineralization experiments. J. Sediment. Res. 83 (1), 37–49.

Ganendra, G., et al., 2014. Formate oxidation-driven calcium carbonate precipitation by *Methylocystis parvus* OBBP. Appl. Environ. Microbiol. 80 (15), 4659–4667.

Given, R.K., Wilkinson, B.H., 1985. Kinetic control of morphology, composition, and mineralogy of abiotic sedimentary carbonates. J. Sediment. Petrol. 55 (1), 109–119.

Greenfield, L.J., 1963. Metabolism and concentration of calcium and magnesium and precipitation of calcium carbonate by a marine bacterium. Ann. N. Y. Acad. Sci. 109, 23–45.

Greinert, J., Derkachev, A., 2004. Glendonites and methane-derived Mg-calcites in the Sea of Okhotsk, eastern Siberia: implications of a venting-related ikaite/glendonite formation. Mar. Geol. 204 (1–2), 129–144.

Gunatilaka, A., Saleh, A., Al-Temeemi, A., Nassar, N., 1984. Occurrence of subtidal dolomite in a hypersaline lagoon, Kuwait. Nature 311 (5985), 450–452.

Hammes, F., Verstraete, W., 2002. Key roles of pH and calcium metabolism in microbial carbonate precipitation. Re/Views Environ Sci. Bio/Technol. 1 (1), 3–7.

Han, X., Suess, E., Sahling, H., Wallmann, K., 2004. Fluid venting activity on the Costa Rica margin: new results from authigenic carbonates. Int. J. Earth Sci. 93 (4), 596–611.

Han, X., et al., 2008. Jiulong methane reef: Microbial mediation of seep carbonates in the South China Sea. Mar. Geol. 249 (3–4), 243–256.

Hauser, L.J., et al., 2011. Complete genome sequence and updated annotation of *Desulfovibrio alaskensis* G20. J. Bacteriol. 193 (16), 4268–4269.

Heuer, V.B., Pohlman, J.W., Torres, M.E., Elvert, M., Hinrichs, K., 2009. The stable carbon isotope biogeochemistry of acetate and other dissolved carbon species in deep subseafloor sediments at the northern Cascadia Margin. Geochim. Cosmochim. Acta 73, 3323–3336.

Hockin, S.L., Gadd, G.M., 2007. Bioremediation of metals and metalloids by precipitation and cellular binding. In: Barton, L.L., Hamilton, W.A. (Eds.), Sulfate-reducing Bacteria. Cambridge University Press, Cambridge, pp. 405–434.

Joye, S.B., et al., 2004. The anaerobic oxidation of methane and sulfate reduction in sediments from gulf of Mexico cold seeps. Chem. Geol. 205 (3–4), 219–238.

Kanaya, K., Okayama, S., 1972. Penetration and energy-loss theory of electrons in solid targets. J. Phys. D. Appl. Phys. 5 (1), 43–58.

Kendall, M.M., et al., 2007. Diversity of archaea in marine sediments from Skan Bay, Alaska, including cultivated methanogens,and description of *Methanogenium boonei* sp. nov. Appl. Environ. Microbiol. 73 (2), 407–414.

Khosrovi, B., Macpherson, R., Miller, J.D.A., 1971. Some observations on growth and hydrogen uptake by *Desulfovibrio vulgaris*. Arch. Microbiol. 80 (4), 324–337.

Kitano, Y., Hood, D.W., 1965. The influence of organic material on the polymorphic crystallization of calcium carbonate. Geochim. Cosmochim. Acta 29 (1), 29–41.

Krause, S., et al., 2012. Microbial nucleation of Mg-rich dolomite in exopolymeric substances under anoxic modern seawater salinity: new insights into an old enigma. Geology 40 (7), 587–590.

Labrenz, M., et al., 2000. Formation of sphalerite (ZnS) deposits in natural biofilms of sulfate-reducing bacteria. Science 290 (5497), 1744–1747.

Larowe, D.E., Dale, A.W., Regnier, P., 2008. A thermodynamic analysis of the anaerobic oxidation of methane in marine sediments. Geobiology 6 (5), 436–449.

Li, X., et al., 2009. A molybdopterin oxidoreductase is involved in H_2 oxidation in *Desulfovibrio desulfuricans* G20. J. Bacteriol. 191 (8), 2675–2682.

Li, X., McInerney, M.J., Stahl, D.A., Krumholz, L.R., 2011. Metabolism of H_2 by *Desulfovibrio alaskensis* G20 during syntrophic growth on lactate. Microbiology 157, 2912–2921.

Lin, Q., et al., 2015. Elemental sulfur in northern South China Sea sediments and its significance. Sci. China Ser. D. 58 (12), 2271–2278.

Liu, R., et al., 2013. Crystallization and oriented attachment of monohydrocalcite and its crystalline phase transformation. Cryst. Eng. Comm. 15 (3), 509–515.

Mann, S., Didymus, J.M., Sanderson, N.P., Heywood, B.R., 1990. Morphological influence of functionalized and non-functionalized-a, w-dicarboxylates on calcite crystallization. J. Chem. Soc. Faraday Trans. 86 (10), 1873–1880.

McGlynn, S.E., Chadwick, G.L., Kempes, C.P., Orphan, V.J., 2015. Single cell activity reveals direct electron transfer in methanotrophic consortia. Nature 526 (7574), 531–535.

Meister, P., 2013. Two opposing effects of sulfate reduction on carbonate precipitation in normal marine, hypersaline, and alkaline environments. Geology 41 (4), 499–502.

Meldrum, F.C., Hyde, S.T., 2001. Morphological influence of magnesium and organic additives on the precipitation of calcite. J. Cryst. Growth 231 (4), 544–558.

Meulepas, R.J.W., Jagersma, C.G., Khadem, A.F., Stams, A.J.M., Lens, P.N.L., 2010. Effect of methanogenic substrates on anaerobic oxidation of methane and sulfate reduction by an anaerobic methanotrophic enrichment. Appl. Microbiol. Biotechnol. 87 (4), 1499–1506.

Morse, J.W., Arvidson, R.S., Luttge, A., 2007. Calcium carbonate formation and dissolution. Chem. Rev. 107 (2), 342–381.

Mucci, A., Morse, J.W., 1983. The incorporation of Mg^{2+} and Sr^{2+} into calcite overgrowths: influences of growth rate and solution composition. Geochim. Cosmochim. Acta 47 (2), 217–233.

Nadson, G.A., 1928. Beitrag zur Kenntnis der bakteriogenen Kalkablagerungen. Arch. Hydrobiol. 19 (1), 154–164.

Nishiyama, R., Munemoto, T., Fukushi, K., 2013. Formation condition of monohydrocalcite from $CaCl_2$–$MgCl_2$–Na_2CO_3 solutions. Geochim. Cosmochim. Acta 100, 217–231.

Oyekola, O., van Hille, R.P., Harrison, S.T.L., 2009. Study of anaerobic lactate metabolism under biosulfidogenic conditions. Water Res. 43 (14), 3345–3354.

Pankhania, I.P., Spormann, A.M., Hamilton, W.A., Thauer, R.K., 1988. Lactate conversion to acetate, CO_2, and H_2 in cell suspension of *Desulfovibrio vulgaris* (Marlburg): indications for the involvement of an energy driven reaction. Arch. Microbiol. 150 (1), 26–31.

Paull, C.K., Chanton, J.P., Neumann, A.C., Coston, J.A., Martens, C.S., 1992. Indicators of methane-derived carbonates and chemosynthetic organic carbon deposits: examples from the Florida escarpment. PALAIOS 7, 361–375.

Plugge, C.M., Zhang, W., Scholten, J.C.M., Stams, A.J.M., 2011. Metabolic flexibility of sulfate-reducing bacteria. Front. Microbiol. 2, 81.

Postgate, J.R., 1984. The Sulphate Reducing Bacteria. Cambridge University Press, Cambridge & London.

Price, M.N., et al., 2014. The genetic basis of energy conservation in the sulfate-reducing bacterium *Desulfovibrio alaskensis* G20. Front. Microbiol. 5.

Reddy, M.M., 1977. Crystallization of calcium carbonate in the presence of trace concentrations of phosphorus-containing anions: I. Inhibition by phosphate and glycerophosphate ions at pH 8.8 and 25 °C. J. Cryst. Growth 41 (2), 287–295.

Rivadeneyra, M.A., Perez-Garcia, I., Salmeron, V., Ramos-Cormenzana, A., 1985. Bacterial precipitation of calcium carbonate in presence of phosphate. Soil Biol. Biochem. 17 (2), 171–172.

Rivadeneyra, M.A., et al., 1993. Precipitation of carbonates by *Bacillus* sp. isolated from saline soils. Geomicrobiol J. 11 (3–4), 175–184.

Rivadeneyra, M.A., Delgado, G., Ramos-Cormenzana, A., Delgado, R., 1998. Biomineralization of carbonates by *Halomonas eurihalina* in solid and liquid media with different salinities: crystal formation sequence. Res. Microbiol. 149 (4), 277–287.

Rivadeneyra, M.A., Párraga, J., Delgado, R., Ramos-Cormenzana, A., Delgado, G., 2004. Biomineralization of carbonates by *Halobacillus trueperi* in solid and liquid media with different salinities. FEMS Microbiol Ecol. 48 (1), 39–46.

Rivadeneyra, M.A., Martin-Algarra, A., Sanchez-Navas, A., Martin-Ramos, D., 2006. Carbonate and phosphate precipitation by *Chromohalobacter marismortui*. Geomicrobiol J. 23 (2), 89–101.

Roberts, W.L., Cambell, T.J., Rapp JR., G.R., 1990. Encyclopedia of Minerals. Van Nostrand Reinhold, New York.

Rodriguez-Blanco, J.D., Shaw, S., Bots, P., Roncal-Herrero, T., Benning, L.G., 2014. The role of Mg in the crystallization of monohydrocalcite. Geochim. Cosmochim. Acta 127, 204–220.

Sanchez-Roman, M., Rivadeneyra, M.A., Vasconcelos, C., McKenzie, J.A., 2007. Biomineralization of carbonate and phosphate by moderately halophilic bacteria. FEMS Microbiol. Ecol. 61 (2), 273–284.

Schulz, H.N., Schulz, H.D., 2005. Large sulfur bacteria and the formation of phosphorite. Science 307 (5708), 416–418.

Stoessell, R.K., 1992. Effects of sulfate reduction on $CaCO_3$ dissolution and precipitation in mixing-zone fluids. J. Sediment. Petrol. 62 (5), 873–880.

Suess, E., 1970. Interaction of organic compounds with calcium carbonate-I. Association phenomena and geochemical implications. Geochim. Cosmochim. Acta 34 (2), 157–168.

Suess, E., 2005. Rv Sonne Cruise Report So 177, Sino-German Cooperative Project, South China Sea Continental Margin: Geological Methane Budget and Environmental Effects of Methane Emissions and Gashydrates.

Suess, E., 2014. Marine cold seeps and their manifestations: geological control, biogeochemical criteria and environmental conditions. Int. J. Earth Sci. 103 (7), 1889–1916 (Geol Rundsch).

Suess, E., et al., 1999. Gas hydrate destabilization: enhanced dewatering, benthic material turnover and large methane plumes at the Cascadia convergent margin. Earth Planet. Sci. Lett. 170 (1–2), 1–15.

Taylor, G.F., 1975. Occurrence of monohydrocalcite in 2 small lakes in Southeast of South Australia. Am. Mineral. 60 (7–8), 690–697.

Thauer, R.K., Stackebrandt, E., Hamilton, W.A., 2009. Energy metabolism and phylogenetic diversity of sulphate-reducing bacteria. In: Barton, L.L., Hamilton, W.A. (Eds.), Sulphate-reducing Bacteria. Cambridge University Press, Cambridge, pp. 1–37.

Tracy, S.L., Williams, D.A., Jennings, H.M., 1998. The growth of calcite spherulites from solution: II. Kinetics of formation. J. Cryst. Growth 193 (3), 382–388.

van Lith, Y., Warthmann, R., Vasconcelos, C., McKenzie, J.A., 2003. Microbial fossilization in carbonate sediments: a result of the bacterial surface involvement in dolomite precipitation. Sedimentology 50 (2), 237–245.

Vasconcelos, C., McKenzie, J.A., 1997. Microbial mediation of modern dolomite precipitation and diagenesis under anoxic conditions (Lagoa Vermelha, Rio de Janeiro, Brazil). J. Sediment. Res. 67 (3), 378–390.

Vasconcelos, C., McKenzie, J.A., Bernasconi, S., Grujic, D., Tien, A.J., 1995. Microbial mediation as a possible mechanism for natural dolomite formation at low-temperatures. Nature 377 (6546), 220–222.

Visscher, P.T., Stolz, J.F., 2005. Microbial mats as bioreactors: populations, processes, and products. Palaeogeogr. Palaeoecol. 219 (1–2), 87–100.

Visscher, P.T., et al., 1998. Formation of lithified micritic laminae in modern marine stromatolites (Bahamas): the role of sulfur cycling. Am. Mineral. 83 (11–12), 1482–1493.
Voordouw, G., 1995. The genus *Desulfovibrio*: the centennial. Appl. Environ. Microbiol. 61 (8), 2813–2819.
Wall, J.D., Rapp-Giles, B.J., Rousset, M., 1993. Characterization of a small plasmid from *Desulfovibrio desulfuricans* and its use for shuttle vector construction. J. Bacteriol. 175 (13), 4121–4128.
Wang, S., Yan, W., Chen, Z., Zhang, N., Chen, H., 2014. Rare earth elements in cold seep carbonates from the southwestern Dongsha area, Northern South China Sea. Mar. Pet. Geol. 57, 482–493.
Warthmann, R., van Lith, Y., Vasconcelos, C., McKenzie, J.A., Karpoff, A.M., 2000. Bacterially induced dolomite precipitation in anoxic culture experiments. Geology 28 (12), 1091–1094.
Wegener, G., Krukenberg, V., Riedel, D., Tegetmeyer, H.E., Boetius, A., 2015. Intercellular wiring enables electron transfer between methanotrophic archaea and bacteria. Nature 526 (7574), 587–590.
Weimer, P.J., Van Kavelaar, M.J., Michel, C.B., Ng, T.K., 1988. Effect of phosphate on the corrosion of carbon steel and on the composition of corrosion products in two-stage continuous cultures of *Desulfovibrio desulfuricans*. Appl. Environ. Microbiol. 54 (2), 386–396.
Wrede, C., et al., 2013. Deposition of biogenic iron minerals in a methane oxidizing microbial mat. Archaea 2013, 102972.
Wright, D.T., 1997. An organogenic origin for widespread dolomite in the Cambrian Eilean Dubh formation, Northwest Scotland. J. Sediment. Res. 67 (1), 54–64.
Wright, D.T., 1999. The role of sulfate-reducing bacteria and cyanobacteria in dolomite formation in distal ephemeral lakes of the Coorong region, South Australia. Sediment. Geol. 126 (1–4), 147–157.
Zullig, J.J., Morse, J.W., 1988. Interaction of organic acids with carbonate mineral surfaces in seawater and related solutions: fatty acid adsorption. Geochim. Cosmochim. Acta 52 (6), 1667–1678.